Available online at www.sciencedirect.com
SCIENCE DIRECT®
Journal of Solid State Chemistry 170 (2003) 435–442
JOURNAL OF SOLID STATE CHEMISTRY
http://elsevier.com/locate/jssc

Sodium "stuffed" $Ba_{2-x}Sr_xFe_4O_8$ ferrites: new cationic conductors

J. Choisnet,* V. Caignaert, and B. Raveau

Laboratoire CRISMAT, UMR CNRS-ISMRA, 6 Boulevard Maréchal Juin, 14050 Caen Cédex, France

Received 25 July 2002; received in revised form 24 October 2002; accepted 5 November 2002

Abstract

Sodium insertion in the tetrahedral layer structure of the ferrites $Ba_{2-x}Sr_xFe_4O_8$ was performed by solid state reaction at 1220 K in air. Superstoichiometric oxides with the actual formula $(Ba_{2-x}Sr_x)_{1-y/4}Na_yFe_4O_8$—$y \leqslant 0.56$; $0.60 \leqslant Ba/Sr \leqslant 1.67$—were characterized by X-ray and neutron powder diffraction. The hexagonal unit-cell volume shows an increasing dependence on the sodium insertion when the Ba/Sr ratio reaches the largest values. The marked expansion of the **c** parameter is the likely signature of the location of the inserted sodium cations within the interlayer space. One-half of the sodium cations partly sits on the Sr(Ba) sites in octahedral coordination and the other half occupies extra octahedral and tetrahedral sites. *ac* conductivity measurements point to a cationic conductivity whose thermally activated regime—$E_a \neq 0.7$ eV—evidenced from 570 K, is unsensitive to the sodium content. The bottleneck of the 2D sodium mobility regards the crossing of the oxygen triangular faces shared by the different polyhedra within the interlayer space.

Keywords: Stuffed ferrites; Tetrahedral layers; Sodium insertion; Cationic conductivity

1. Introduction

Recently, the new ferrites $Ba_{2-x}Sr_xFe_4O_8$ have been prepared [1]. Their structure consists of double layers of FeO_4 tetrahedra, connected by octahedra which partly fill the interlayer space (Fig. 1). The formation of a rather large homogeneity range of solid solution—$0.54 \leqslant Ba/Sr \leqslant 1.5$—is ensured by the existence of a partial disorder in the distribution of the Ba^{2+} and Sr^{2+} cations in the centers of the crowns—12-fold coordination—and in the octahedra. As a member of the tridymite-like structures, the $BaSrFe_4O_8$ type [2,3] has a relatively low tetrahedral framework density of 19.3 tetrahedral ions (T) per 1000 $Å^3$ [4]. This value compares rather well with those of the corresponding silicates: from 22.6 T for tridymite toward the minimum value of 12.7 T for the faujasite zeolite [4]. Consequently, the $BaSrFe_4O_8$ type is expected to exhibit the typical properties of the so-called stuffed derivatives of silica, for example some extent of cationic mobility.

In order to check the occurrence of such a property, it was decided to investigate the insertion of sodium cations in the ferrites $Ba_{2-x}Sr_xFe_4O_8$. In the following, we report on the successful attempt in preparing superstoichiometric compounds with the formula $(Ba_{2-x}Sr_x)_{1-y/4}Na_yFe_4O_8$. The crystal chemistry of these oxides is described from the results of an X-ray powder diffraction (XRPD) and neutron powder diffraction (NPD) combined study. The existence of a mobility of the sodium cations is discussed on the basis of the data of *ac* conductivity measurements and a mobility pathway is proposed.

2. Experimental

Appropriate mixtures of barium, strontium, sodium carbonates and iron(III) oxide were heated in air, in alumina crucibles, first at 870 K for 6 h. After a regrinding, an annealing at 1220 K for 6 h, followed by an air-quenching, was performed.

Seventeen as-prepared samples were characterized by XRPD. Diffractograms were recorded in the angular range 6–120°2θ on a Philips vertical goniometer equipped with a secondary graphite monochromator (Cu$K\alpha$ radiation). The cationic composition of four samples was determined by energy dispersive spectroscopy (EDS) using an analyser mounted on a JEOL 200CX electron microscope. In the case of the actual

*Corresponding author. Fax: +33-2-31951600.
E-mail address: jacques.choisnet@ismra.fr (J. Choisnet).

0022-4596/03/$ - see front matter © 2002 Elsevier Science (USA). All rights reserved.
doi:10.1016/S0022-4596(02)00136-6

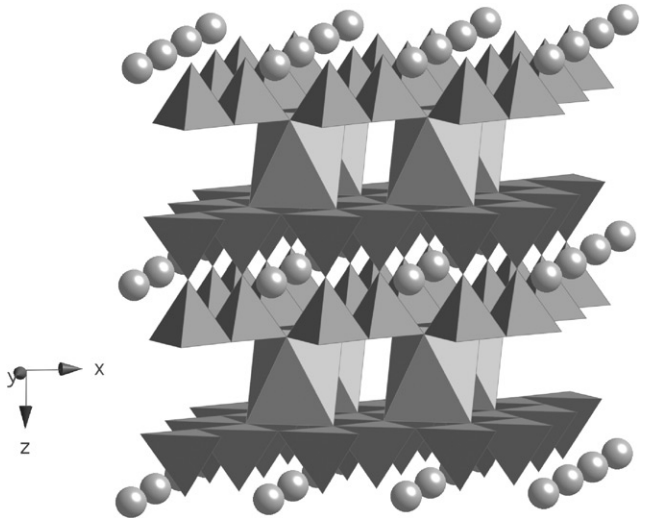

Fig. 1. Perspective view of the structure of the ferrites $Ba_{2-x}Sr_xFe_4O_8$: Ba(Sr) occupy the centers of the crowns formed by the (Fe_4O_8) double tetrahedral layers. The interlayer space is partly filled by Sr(Ba) octahedra.

composition $Ba_{1.04}Sr_{0.74}Na_{0.44}Fe_4O_8$, NPD data were collected at room temperature in the angular range 6–126°2θ, on the G41 diffractometer at the LLB, Saclay, France ($\lambda = 2.4266$ Å). NPD and XRPD data of this composition were combined in a Rietveld structure analysis of both the geometrical and the magnetic structures, Fullprof code [5].

Electrical measurements of five compositions were performed on cylindrical disks ($d = 8$ mm, $e = 1$ mm) compacted under 300 bars and sintered at 1220 K in air. A silver paste was painted on the disk faces and heated up to 870 K. Impedance measurements were performed by using a EGG 5209 video bridge in the range 20 Hz–120 kHz.

3. Results and discussion

3.1. Range of existence of the compositions $(Ba_{2-x}Sr_x)_{1-y/4}Na_yFe_4O_8$

The formation of sodium-inserted ferrites was observed in a wide range of compositions, namely: $0.60 \leqslant Ba/Sr \leqslant 1.67$ and nominal values of $y \leqslant 1.15$. The extent of barium–strontium replacement compares well with that of the parent ferrites $Ba_{2-x}Sr_xFe_4O_8$ ($0.54 \leqslant Ba/Sr \leqslant 1.5$). Note only a small shift of the Ba/Sr ratio toward the barium-rich values.

The problem of the actual amount of sodium present in the inserted ferrite was considered from the results of the EDS analysis of four nominal compositions, $y = 0.4$, 0.6, 0.9 and the limiting value 1.15. Approximately 20 microcrystals of each composition were retained. First of all, it was checked that the presence of any element other than Ba, Sr, Na and Fe was never detected. This allows to rule out the incorporation of aluminum from the crucible, occurring during the synthesis. Table 1 reports the nominal and actual values of their sodium content together with the corresponding values of their nominal and actual Ba/Sr ratio. Clearly, the actual value of the Ba/Sr ratio is rather close to the nominal one, whereas the actual sodium content, $\mathbf{y}_a$, is significantly lower than the nominal one, y. The systematic presence of microcrystals of extra phases was observed, namely $NaFeO_2$ and iron oxides, in agreement with the NPD phase analysis. Assuming that the Ba/Sr ratio remains unchanged and the actual sodium content is the half of the nominal one, a tentative calculation of the percentage of inserted sodium ferrite to be formed was undertaken. In any case, the minimum value of this percentage, calculated as equal to 100 $(1-y/4)/(1+y/4)$, is always larger than 50%, i.e. 55% for the limiting nominal value $y = 1.15$.

Table 1
Nominal and actual values of the sodium content and the Ba/Sr ratio in the sodium-inserted ferrites $(Ba_{2-x}Sr_x)_{1-y/4}Na_yFe_4O_8$ (from EDS results)

Sodium content		Ba/Sr ratio	
Nominal y	Actual y_a	Nominal	Actual
0.40	0.18	1.25	1.22
0.60	0.30	1.43	1.40
0.90	0.44	1.38	1.40
1.15	0.56	1.38	1.36

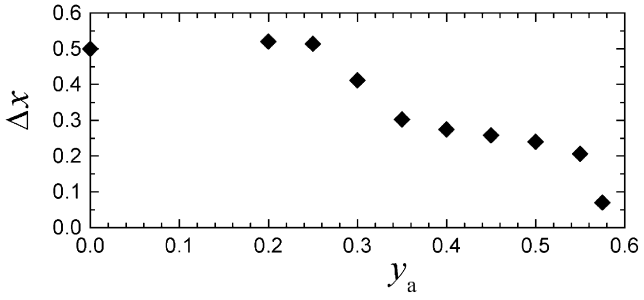

Fig. 2. Variation of the barium–strontium balance Δx_{Ba-Sr} versus the actual sodium content y_a.

The main interesting feature regarding the existence of these sodium-inserted ferrites is the mutual dependence of the mechanism of sodium insertion and the barium for strontium substitution. Fig. 2 gives the variation of the barium–strontium balance versus the actual value of inserted sodium y_a. Δx_{Ba-Sr} is the value of the maximum extent of the Ba–Sr replacement, for a given value of y_a, in the formula $(Ba_{2-x}Sr_x)_{1-y_a/4}Na_{y_a}Fe_4O_8y_a$, the actual value of inserted sodium is considered as equal to half of the nominal one y. Up to $y_a = 0.25$, Δx_{Ba-Sr} remains close to the maximum value 0.5 observed in the parent ferrites $Ba_{2-x}Sr_xFe_4O_8$. Then it decreases first strongly

and soon afterward smoothly, to the value 0.2 for $y_a = 0.55$. A further increase of y_a results in a vanishing of the barium for strontium substitution. In this respect, it has to be noticed that any attempt to prepare sodium-inserted ferrites from mixtures with nominal sodium contents $y > 1.15$ was unsuccessful.

3.2. Hexagonal cell constants: dependence on the inserted sodium

The diffractograms of all the as-prepared samples were indexed in the $BaSrFe_4O_8$-type hexagonal cell. The values of $\mathbf{a}_h$ and $\mathbf{c}_h$ show a variation which depends both on the amount of inserted sodium and the barium–strontium replacement. The extent of variation of $\mathbf{a}_h$ is small, $\Delta a_h = 0.01$ Å, and remains equal to that found for the parent ferrites $Ba_{2-x}Sr_xFe_4O_8$ [1]. Conversely, Δc_h is larger: 0.09 Å instead of 0.06 Å. This anisotropical effect can be understood as the signature of an increasing amount of sodium. More in detail, one can separate the respective contributions of the barium–strontium replacement and the sodium insertion. In Fig. 3 is considered the variation of the hexagonal unit-cell volume $\mathbf{V}_h$ of the compositions $(Ba_{2-x}Sr_x)_{1-y_a/4}Na_{y_a}Fe_4O_8$, versus the Ba/Sr ratio $(2\text{-}x)/x$, in a comparison with the parent ferrites $Ba_{2-x}Sr_xFe_4O_8$. For the low values of the Ba/ Sr ratio—Ba/Sr $\leqslant 0.94$—there is no supplementary expansion of the structure to be due to the sodium insertion. This is no longer true for larger values of the Ba/Sr ratio: the unit-cell volume of the sodium-inserted ferrites increases with respect to the parent ferrite and this is more and more pronounced for the largest values of the Ba/Sr ratio. Finally, it has to be emphasized that the insertion of sodium cations makes easier the substitution of barium for strontium, resulting in a shift of the homogeneity range of the compositions $(Ba_{2-x}Sr_x)_{1-y_a/4}Na_{y_a}Fe_4O_8$ toward larger values of the Ba/Sr ratio, $(Ba/Sr)_{max} \# 1.67$ instead of 1.5 in the parent ferrites. This fact is of importance for the structural study, namely in order to find the most likely location of the sodium cations in the tetrahedral structure.

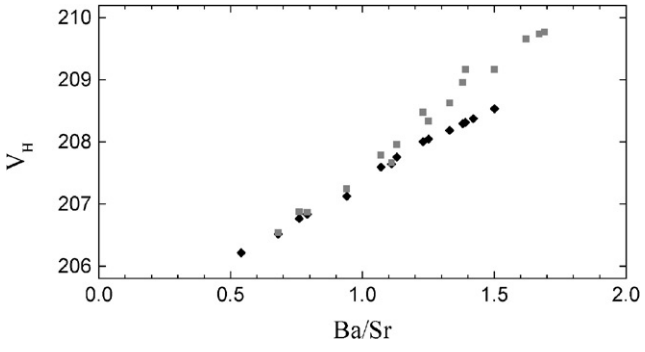

Fig. 3. Variation of the hexagonal unit-cell volume V_h versus the Ba/Sr ratio in the sodium-inserted ferrites (gray squares) and for comparison, in $BaSrFe_4O_8$ (black symbols).

3.3. Structure calculations: location of the inserted sodium cations

Structure calculations of the actual composition $Ba_{1.04}Sr_{0.74}Na_{0.44}Fe_4O_8$ were carried out in terms of a combined XRPD and NPD study. The NPD data were recorded in the range 6–126°2θ with a step size 0.05°2θ. The presence of the extra phases $NaFeO_2$, α-Fe_2O_3 corundum and Fe_3O_4 magnetite, was introduced in the NPD calculations but not in the XRPD one, where the extra peaks are too weak to be detected. The XRPD data were recorded by using specific experimental parameters in three angular ranges: 10–62°2θ, step size 0.02°2θ; 62–120°2θ, step size 0.03°2θ and 120–140°2θ, step size 0.04°2θ.

Concerning the NPD data, the as-recorded diffractogram includes the contribution of the magnetic structure, as evidenced from the presence of several supplementary reflections. In agreement with the early data reported on the antiferromagnetism of $BaSrFe_4O_8$ [2], these magnetic reflections can be indexed on the basis of a hexagonal cell identical to the geometrical one, which result points to a propagation vector $k = \{0,0,0\}$. The NPD refinement calculation was performed with iron atoms labelled in the following way : (1) 1/3, 2/3, z (2) 1/3, 2/3, $-z$ (3) 2/3, 1/3, $-z$ (4) 2/3, 1/3, z. Several models were checked but the only model that is able to reproduce the experimental data is given by a G-type structure, i.e. $\mathbf{S_1}$–$\mathbf{S_2}$ + $\mathbf{S_3}$–$\mathbf{S_4}$, following the notation of Bertaut with moments aligned along the **c**-axis. The value of the iron magnetic moment (3.2 μ_B) is compatible with Fe^{3+} and is consistent with the existence of antiferromagnetic interactions along the **c**-axis and in the (**a,b**) plane. Although the double tetrahedral layers are connected to each other by non-magnetic atoms, the magnetic ordering is well ensured along the **c** direction.

The main goal of the structure calculations regarded the presence and the location of the sodium cations inserted in the tetrahedral layer structure of $BaSrFe_4O_8$. Due to intrinsic limitations, one could not expect to propose a fully unambiguous answer to this problem. In this respect, the existence of extra phases, which was taken into account in the Rietveld procedure, was assumed not to prevent to get meaningful results. As a matter of fact, their calculated overall amount never exceeds 15%, in agreement with the value 18% deduced from a phase composition analysis. The true difficulty concerned the crystal–chemical models to be used for the location of sodium cations. First of all, it has to be stated that the chemical inhomogeneity does not concern this problem. It is a usual property of the open structures to exhibit several possible sites for the location of the inserted atoms, no one being strongly

energetically favored. It is why the contribution of the air-quenching to a supplementary disorder of the inserted ions is likely to be negligible. In the structure of $BaSrFe_4O_8$, beside the sites which are occupied, i.e. the centers of the crowns and the octahedral sites which connect the double layers, some extra site(s) have to be considered, as a logical consequence of the super-stoichiometric sodium composition. In this respect, there are only two fully different ways:

(i) the whole sodium cations sit within the crowns—the $[Ba,Sr,Na]^{XII}$ sites—on the basis of the presence of two sodium cations in the free void due to the absence of one barium (strontium) cation, i.e. the structural formula $[Ba_{0.78-u}Sr_uNa_{0.44}]^{XII}$ $[Sr_{0.74-u}Ba_{0.26+u}]^{VI}Fe_4O_8$;

(ii) one-half of the sodium cations sit in the interlayer octahedra replacing strontium(barium) cations—the $[Sr,Ba,Na]^{VI}$ sites—while another half occupy some octahedral X_{oc} or(and) tetrahedral X_t extra sites in the interlayer space, as visible in Fig. 4a and 4b. The structural formula is: $[Ba_{1-u}Sr_u]^{XII}$ $[Sr_{0.74-u}Ba_{0.04+u}Na_{0.22}]^{VI}$ $[Na_{0.22}]^{X_{oc},X_t}Fe_4O_8$.

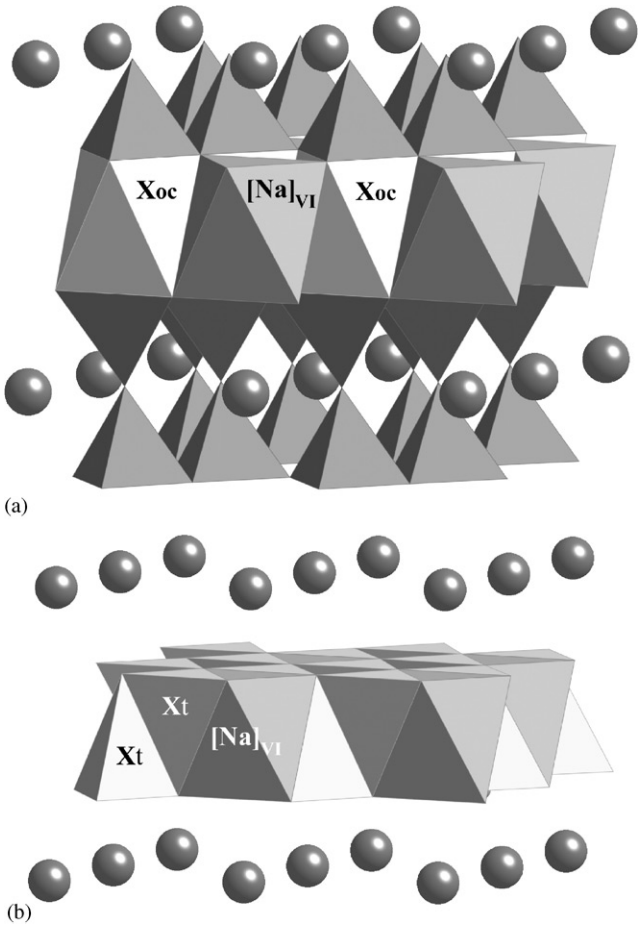

Fig. 4. Extra sites with respect to the octahedral $[Na]^{VI}$ in the interlayer space: (a): octahedral X_{oc} sites; (b): tetrahedral X_t sites (the FeO_4 tetrahedra are omitted).

The Rietveld refinement procedure was based on the $BaSrFe_4O_8$ model, S.G. $P\bar{3}1m$ [2]. *The first set of calculations* regarded the case of the location of the whole sodium cations within the crowns. In agreement with the existence of a weak and diffuse residual density, approximately 10% of the Ba(Sr) peak, a tentative position of Na at 1.3 Å from the center of the crown, $x \# 0.09$; $y \# 0.23$; $z \# 0.09$, was considered. After refining first all the variable parameters, except the position and the isotropic B thermal factor of Na and then, the position and the B factor of Na, a convergence was reached: RB_N, R_{magn}, RB_{X1} RB_{X2} RB_{X3} equal to 6.7, 8.9, 7.6, 8.2, 10.0, respectively. The calculated interatomic distances concerning the sodium atoms are not realistic, as for example, one Na–O distance which is close to 2 Å. Consequently, the presence of the whole sodium cations within the crowns, as a result of the replacement of one barium by two sodium cations, should be ruled out. The diffuse residual electron density is more likely to be ascribed to a large anisotropic motion of the barium cations.

The second set of calculations took into account the presence of sodium cations in the interlayer space. An examination of the interatomic distances in the two types of interlayer extra sites, the X_{oc} and X_t sites, gives the following values:

—the six X_{oc}—O distances are equal to 2.51 Å, i.e. rather large values for sodium cations in octahedral coordination. Simultaneously, there are two apical X_{oc}—Fe distances close to 2.22 Å: one can suppose that they will not trigger so strong repulsive forces, if we keep in mind that a significant screening of the electrostatic repulsions will occur, as a result of the oxygen face sharing by the (NaO_6) X_{oc} site and the (FeO_4) tetrahedron (Fig. 4a).

—in the tetrahedral X_t site, the mean Na–O distance is rather short, 2.26 Å, as the average of the four values : 2.12–2 × 2.25 Å and 2.40 Å. Due to a face sharing of the X_t sites with the $[Sr,Ba,Na]^{VI}$ sites (Fig. 4b), the simultaneous occupation of these two sites is not possible, X_t.

—$[Sr,Ba,Na]^{VI} \# 1.75$ Å. Consequently, the occupation of the X_t sites by sodium cations has to be paired with the existence of a sodium vacancy in the $[Sr,Ba,Na]^{VI}$ site.

On the basis of these observations, it was decided to check, at first, the occupation of the X_{oc} sites and then, the coupled occupation of the X_{oc} and X_t sites. In both cases, the calculation procedure was the same. Starting from the $BaSrFe_4O_8$ model as a first step, the likely positions of Na were derived from the results of the NPD Fourier analysis. The structural formulas and the corresponding positions of Na are as follows:

$[Ba_{1-u}Sr_u]^{XII}$ $[Sr_{0.74-u}Ba_{0.04+u}$ $Na_{0.22}]^{VI}$ $[Na_{0.22}]^{X_{oc}}Fe_4O_8$, X_{oc} in: $x \# 0.33$; $y \# 0.67$; $z \# 0.50$, $[Ba_{1-u}Sr_u]^{XII}$ $[Sr_{0.74-u}Ba_{0.04+u}$ $Na_{0.11}\square_{0.11}]^{VI}$ $[Na_{0.22}]^{X_{oc}}[Na_{0.11}]^{X_t}$

Fe_4O_8, X_{oc} as above and X_t in: $x \# 0.31$; $y = 0.0$; $z \# 0.54$.

The starting value $u = 0.18$, derived from $BaSrFe_4O_8$ [1], was retained in both cases.

After refining the positional variables and the isotropic thermal factors of all the atoms except those of sodium which remained fixed, the Ba/Sr balance, variable u, was introduced in the calculation. Then, a tentative variation of the atomic coordinates of the sodium cations was considered: only the variables y_{oc} and x_t can be calculated. The corresponding results are:

—X_{oc} sites: a large shift from the starting position was calculated, 0.60 Å. This results in a lengthening of the two Na_{oc}–Fe distances: 2.22 → 2.31 Å and a splitting of the set of six Na_{oc}–O distances, 2.51 Å, in three longer ones: 2.99, 2.80, 2.79 Å and three shorter ones: 2.36, 2.35, 2.10 Å

—X_t sites: no significant shift was calculated. Consequently, the four Na_t–O distances are very close to the starting values : 2.11, 2 × 2.26 and 2.32 Å.

A convergence was reached for the final values of the variable parameters reported in Table 2. In this last calculation procedure, the isotropic thermal factors of the sodium cations were taken into account. The first model which corresponds to an occupation of the X_{oc} sites only, has a slightly better confidence. The experimental, calculated and difference NPD patterns of this model are plotted in Fig. 5. As expected, the values of the overall set of atomic parameters and their standard deviations as well, are nearly unsensitive to the different occupations of the X_{oc} and X_t sites. In both models, large values of B_{Na}, the thermal factors of inserted sodium cations, were calculated. Certainly, due to the constraints which were applied, a precise discussion of the meaning of B_{Na} is not possible. However, one has to bear in mind that in the open structures of superionic conductors, abnormally large values of the thermal factors of inserted cations are systematically found: for example, in 1D titanogallates of alkaline cations, B_K, B_{Rb}, B_{Cs} are equal to 8.0–9.2 and 11.1 $Å^2$, respectively [6] and in 1D quadruple rutile chain structures of sodium ferrititanates the calculated value of B_{Na} is 5.5 $Å^2$ [7]. In this respect, the value 7.8 $Å^2$ calculated for B_{Na} in the X_{oc} sites is likely to be related to a potential mobility of the sodium cations in these new phases.

To sum up the different results of this structural study, it is useful to give a statement of the information obtained on the structure of the ferrite $Ba_{1.04}Sr_{0.74}Na_{0.44}Fe_4O_8$, according to their degree of certainty. At first, the insertion of the sodium cations occurs in the interlayer space, i.e. between the double tetrahedral layers and not within the crowns. This was the rather likely hypothesis to be based on the anisotropic increase of the c parameter of the unit cell. It is undoubtedly ensured by the results of the structure calculations. In any case, a half of the inserted sodium will be found in some supplementary distorted octahedral sites (X_{oc}). The other half will be substituted for strontium (barium) cations in octahedral coordination. However, it cannot be precluded that a part of these sodium cations, at best the half, will leave this Sr(Ba) octahedral sites in order to occupy some neighboring distorted tetrahedral sites (X_t). This structural scheme, namely the simultaneous occupation of X_{oc} and X_t sites seems to be possible, as it will allow the compression of the Na–O bonding in tetrahedral coordination to be relaxed by the Na–O underbonding in octahedral coordination. This is visible in a simple way from the calculated mean value of the X_{oc}–O distances and X_t–O distances which is equal to 2.41 Å.

Table 2
Atomic parameters of the structure of the composition $Ba_{1.04}Sr_{0.74}Na_{0.44}Fe_4O_8$, SG $P\bar{3}1m$, as obtained from a combined NPD and XRPD Rietveld analysis

At. Param.	Model[a]	Model[b]	At. Param.	Model[a]	Model[b]
u	0.18(2)	0.17(2)	X_{oc}	$Na_{0.22}$	$Na_{0.22}$
(XII) occup.	$Ba_{0.82}/Sr_{0.18}$	$Ba_{0.83}/Sr_{0.17}$	y	0.55(1)	0.55(1)
(XII) B $(Å)^2$	1.26(8)	1.29(8)	X_{oc} B $(Å)^2$	7.8(3)	4.6(2)
(VI) occup.	$Sr_{0.56}/Ba_{0.22}$	$Sr_{0.57}/Ba_{0.21}$	X_t	—	$Na_{0.11}$
	$Na_{0.22}$	$Na_{0.11}\square_{0.11}$	x	—	0.318(3)
(VI) B $(Å)^2$	0.29(7)	0.10(7)	X_t B $(Å)^2$	—	3.3(2)
Fe z	0.2269(2)	0.2270(2)	O_2 x	0.3399(6)	0.3398(6)
Fe B $(Å)^2$	0.53(2)	0.54(2)	O_2 z	0.2853(3)	0.2854(3)
O_1 B $(Å)^2$	1.40(7)	1.43(7)	O_2 B $(Å)^2$	1.12(3)	1.15(3)

Two structural models are reported.

[a] $[Ba_{1-u}Sr_u]^{XII}$ $[Sr_{0.74-u}Ba_{0.04+u}$ $Na_{0.22}]^{VI}$ $[Na_{0.22}]^{X_{oc}}Fe_4O_8$. R factors, NPD: $R_B = 0.064$, $R_P = 0.144$, $R_{WP} = 0.119$, $R_{magn} = 0.049$. XRPD: R_B for the three angular ranges (1) 0.052, (2) 0.063, (3) 0.079.

[b] $[Ba_{1-u}Sr_u]^{XII}$ $[Sr_{0.74-u}Ba_{0.04+u}$ $Na_{0.11}\square_{0.11})^{VI}$ $[Na_{0.22}]^{X_{oc}}[Na_{0.11}]^{X_t}Fe_4O_8$. R factors, NPD: $R_B = 0.068$, $R_P = 0.146$, $R_{WP} = 0.120$, $R_{magn} = 0.052$. XRPD: R_B for the three angular ranges (1) 0.057, (2) 0.064, (3) 0.073. The different sets of atomic positions are: 1a (0,0,0) for $[Ba, Sr]^{XII}$; 1b (0,0,1/2) for [Ba, Sr, Na]^{VI}; 2c (1/3, 2/3, 0) for O_1; 4h (1/3, 2/3, z) for Fe; 6k (x, 0, z) for O_2 and $[Na]^{X_t}$ with $z = 0.545$(fixed); 12l (x, y, z) for $[Na]^{X_{oc}}$ with $x = 1/3$(fixed) and $z = 1/2$(fixed).

4. ac conductivity measurements: evidence for Na^+ mobility

Four compositions of sodium-inserted ferrites—actual values $y_a = 0.25$, 0.4, 0.45, 0.5 and $BaSrFe_4O_8$ for comparison, were retained for *ac* conductivity measurements in the temperature range RT → 875 K. As an example, the complex impedance plots of the actual composition $Ba_{0.93}Sr_{0.82}Na_{0.5}Fe_4O_8$, at three temperatures, are shown in Fig. 6. Semicircles are systematically observed within the experimental temperature range. The ionic contribution to the conductivity was obtained by extrapolation of the low-frequency region of the semicircles to the real axis. The conductivity of $Ba_{1.07}Sr_{0.8}Na_{0.25}Fe_4O_8$, the smallest actual value y_a herein considered, is close to $10^{-6}\,S\,cm^{-1}$ at 630 K: this temperature is assumed to correspond to the beginning of the ionic conductivity regime for $y_a = 0.25$. The value of this limiting temperature decreases as a function of the sodium amount. In the best case, namely the composition $y_a = 0.5$, the ionic conductivity exists from 570 K, $S \# 10^{-5}\,S\,cm^{-1}$. In the parent ferrite $BaSrFe_4O_8$, composition $y_a = 0$, a conductivity close to $3 \times 10^{-7}\,S\,cm^{-1}$ was measured at 730 K. This value is approximately 1000 times weaker than the corresponding conductivity measured in the composition $y_a = 0.5$. One can deduce from this information that the contribution of the electronic conductivity which is logically expected to occur in any ferrite, is very low and consequently, the sodium-inserted ferrites herein

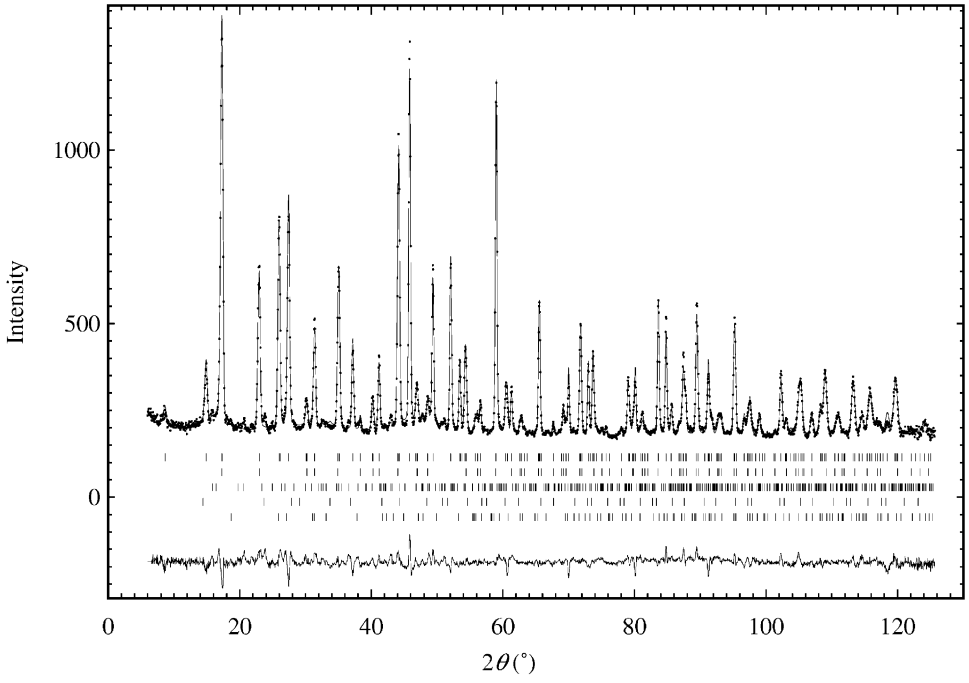

Fig. 5. Experimental (dots), calculated (lines) and difference NPD patterns of $Ba_{1.04}Sr_{0.74}Na_{0.44}Fe_4O_8$. Vertical bars indicate, respectively, the whole reflections of the title phase, the magnetic contribution, the extra phases $NaFeO_2$, Fe_3O_4 and α-Fe_2O_3.

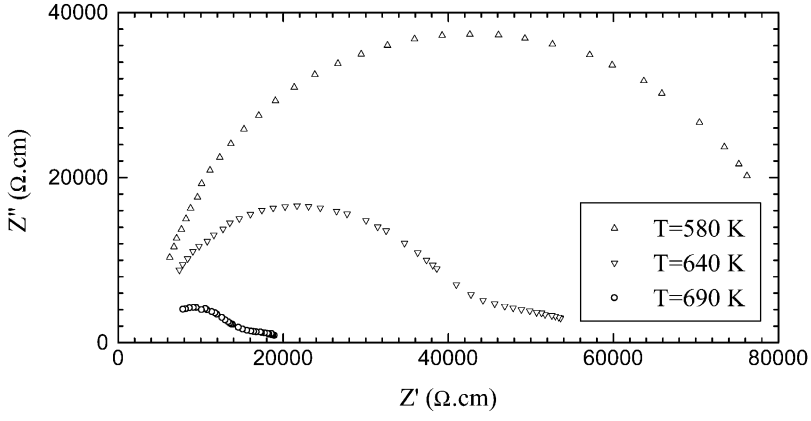

Fig. 6. Complex impedance plots obtained for the actual composition $Ba_{0.93}Sr_{0.82}Na_{0.5}Fe_4O_8$ at three temperatures.

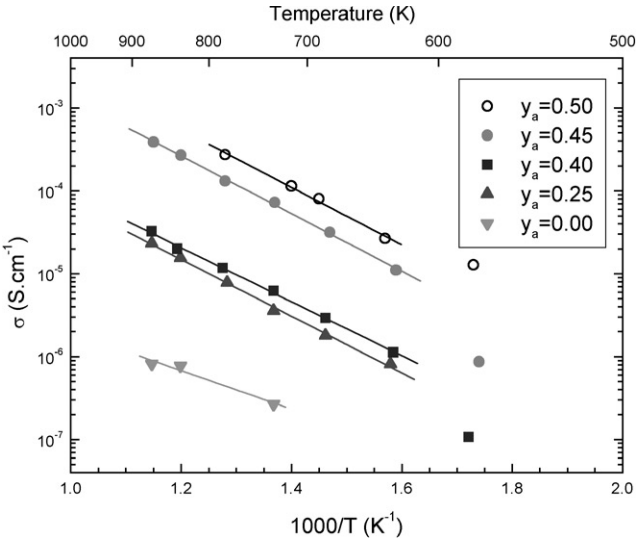

Fig. 7. Logarithmic plots of the conductivity σ versus $1000/T$ obtained in four sodium-inserted ferrites (y_a = actual sodium content) and $BaSrFe_4O_8$ ($y_a = 0$).

studied can be reasonably considered as cationic conductors.

The total *ac* conductivity σ was considered in its dependence on the temperature. As the experimental temperature range of ionic conductivity is rather small, 570 → 870 K, it was decided to plot $\log(\sigma)$ versus $(10^3/T)$. Fig. 7 shows that a linear regime is systematically observed. The linear plots rank well versus y_a, i.e. the total conductivity increases regularly: in the best case, $y_a = 0.5$, the conductivity increases from 3×10^{-5} to 3×10^{-4} S cm^{-1} in the range 630 → 780 K. In the non-inserted structure of $BaSrFe_4O_8$, the low level of conductivity, not larger than 10^{-6} S cm^{-1} at 870 K, is ascribed to the contribution of the electronic conductivity $E_a \# 0.45$ eV. Remarkably, the activation energy of the cationic conductivity is constant and equal to 0.69(2) eV, whatever y_a composition is considered. This is the proof that a well-defined mechanism of cationic mobility occurs in these sodium-inserted ferrites.

As deduced from the structure analysis, the whole amount of inserted sodium cations is found in the interlayer space where they occupy three sites, namely the $[Sr,Ba,Na]^{VI}$ sites and the X_{oc} and X_t extra sites. A mobility pathway within the interlayer space can be proposed (Fig. 8a):

—starting from a [VI] site (1), a sodium cation reaches first one of the six nearest tetrahedral X_t sites;

—then, from a X_t site it moves toward one of the two possible octahedral X_{oc} sites (2) and further, one of the five surrounding X_t sites (3);

—as a last step, the sodium cation leaves the latter X_t site to join either a [VI] site (4), from which position a cyclic mechanism will occur.

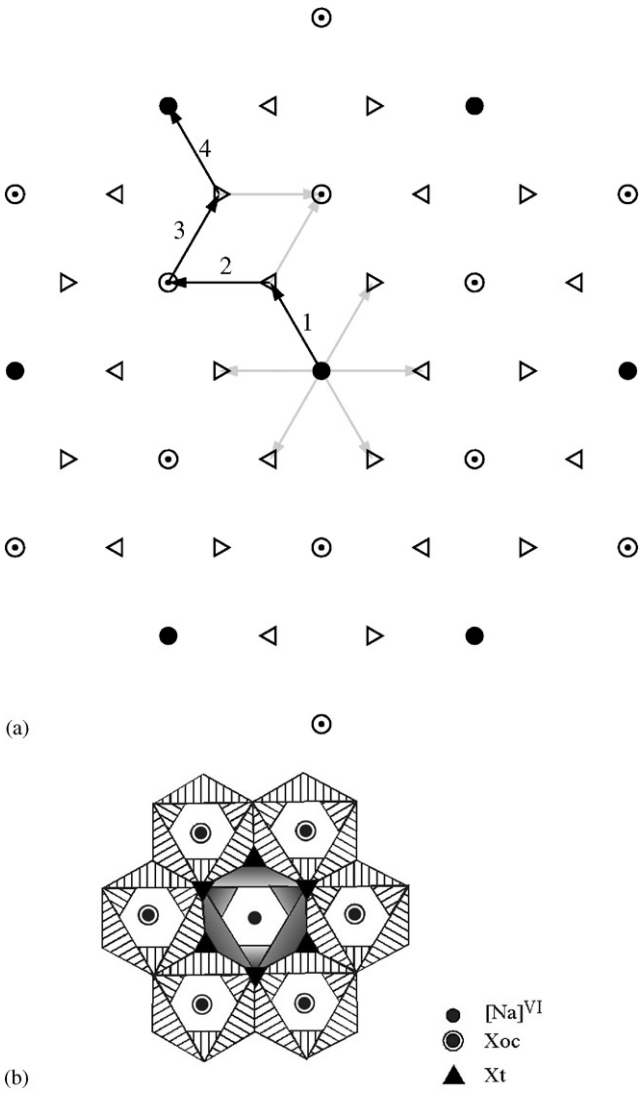

Fig. 8. Mobility pathway of sodium cations in the interlayer space: (a): black circles, open triangles and circles feature, respectively, the [VI], X_t and X_{oc} sites; (b): oxygen triangular faces shared by a $[Na]_{VI}$ and a X_t site (gray) and by a X_t and a X_{oc} site (hatched).

In any case, such a mobility pathway requires the crossing of oxygen triangular faces shared by these polyhedra (Fig. 8b). In this respect, there are only two different cases: the triangular face shared by a $[Na]^{VI}$ and a X_t site and the triangular face shared by a X_t and a X_{oc} site. The calculated distances between the center of these triangles and their apices are 2.16 Å and 2.14 Å, respectively. These values are shorter than the usual one for the Na–O distance which is close to 2.4 Å. Clearly, one has to see in these data the "bottleneck" of the mobility pathway. Under these conditions, the cationic conductivity cannot occur at RT and the activation energy ($E_a \# 0.7$ eV) is not as low as in typical Na^+ ionic superconductors: 0.16 eV in sodium β-aluminas [8], 0.20 eV in quadruple rutile chain sodium ferritianantes [7]. On the contrary, these sodium-inserted tetrahedral

ferrites well compare with the alluaudite-type sodium complex phosphate $Na_2FeMn_2(PO_4)_3$ [9]: in that case, the activation energy of the sodium mobility in the channels of the mixed tetrahedral–octahedral structure is close to 0.77 eV. In the same way, the value reported for the conductivity σ at 750 K, 8×10^{-5} S cm^{-1} [9] is not very different from the value 3×10^{-4} cm^{-1} we obtained for the composition $y_a = 0.5$.

Finally, it must be emphasized that a further extension of the dimensionality of the mobility pathway seems to be precluded. As a matter of fact, a migration of the sodium cations across the triangular face of the X_t site which is perpendicular to the z-axis is strongly hindered since the calculated distance for the "bottle-neck" is 1.80 Å. These sodium-inserted ferrites are typical 2D cationic conductors. The mobility concerns the interlayer space, it cannot be extended to the double tetrahedral layers.

5. Concluding remarks

We have demonstrated for the first time, the possibility to interpolate additional cations in the $BaSrFe_4O_8$-type structure. Such a property is in agreement with the close relationships of this structural type with the silica-like tretrahedral oxides which exhibit a great ability to form stuffed derivatives. The originality of these superstoichiometric tetrahedral oxides with respect to stuffed derivatives of silica deals with the insertion of sodium cations in the interlayer space, the large sites within the crowns remaining fully occupied by barium and strontium cations. As a result, sodium cations sit for 50% in the octahedral Sr(Ba) sites and for 50% in new distorted octahedral and tetrahedral sites. Such a cationic distribution generates for these Na-stuffed ferrites some extent of bidimensional cationic mobility. The latter is indeed significant at temperatures higher than 570 K. The extra tetrahedral sites are likely to take a prominent part because they allow a migration both toward "nominal" and extra octahedral sites, within the interlayer space, the displacement in the perpendicular direction being sterically hindered. This study opens the route to the generation of new stuffed tetrahedral frameworks which rank apart from the numerous silica like oxides.

Acknowledgments

The authors are grateful to Dr. F. Bourrée for the neutron diffraction data collection.

References

[1] J. Choisnet, B. Raveau, J. Mater. Chem. 12 (2002) 1005.
[2] D. Hermann-Ronzaud, M. Bacmann, Acta Crystallogr. B 31 (1975) 665.
[3] M.C. Cadée, Acta Crystallogr. B 31 (1975) 2012.
[4] F. Liebau, Structural Chemistry of Silicates, Springer Berlin, Heidelberg, p. 155, 1985.
[5] J. Rodriguez-Carvajal, Program Fullprof 3.5, 1997.
[6] M. Watanabé, Y. Fujiki, S. Yoshikado, T. Ohachi, Solid State Ionics 28/30 (1988) 257.
[7] F. Archaimbault, J. Choisnet, J. Solid State Chem. 90 (1991) 216.
[8] S. Chandra, Superionic Solids, North-Holland, Amsterdam, p. 53, 1981.
[9] A. Daidouh, C. Durio, C. Pico, M.L. Veiga, N. Chouaibi, A. Ouassini, Solid State Sciences 4 (2002) 541.